

FABRICATION AND CHARACTERIZATION OF  
ACTIVATED CARBON / GRAPHENE  
SUPERCAPACITOR AS AN ENERGY STORAGE  
DEVICE AND ITS EQUIVALENT CIRCUIT MODEL

BY

ABDUL HAKIM BIN AB. RAHIM

A thesis submitted in fulfillment of the requirement for the  
degree of Doctor of Philosophy (Engineering)

Kulliyyah of Engineering  
International Islamic University Malaysia

JUNE 2022

## ABSTRACT

This thesis presents the investigations of graphene materials' contribution when used in combination with the traditional supercapacitor electrode material, the Activated Carbon (AC). The analyses were conducted via material characterization and electrochemical characterization methods. The study also proposed a new Equivalent Circuit Model (ECM) that can be used as another characterization approach besides producing a better supercapacitor model in a virtual electronic system environment. Literature works show that a small amount of graphene addition on the AC electrode enhanced the performance of the electrode in an improved specific capacitance and lowered the internal resistance. However, some researchers reported that further graphene addition would offset the improvement as graphene typically has a lower specific surface area compared to the AC. This work explores the performance of supercapacitor electrodes with pure AC, pure graphene, and several AC-graphene composites ratios. Two types of graphene were used, two-dimensional graphene using Graphene Nanoplatelets (GNP) and three-dimensional graphene using Graphene Aerogel (GA). It was found that increasing GNP wt% in the electrode would increase the prototype's specific capacitance in a linear relationship, with an insignificant effect on the internal resistance. On the other hand, 20 wt% GA on the electrode performs the best capacitance among the GA-based prototypes, while further GA wt% increase decreases the capacitance. Higher internal resistances were also recorded with higher GA wt%. Besides the capacitance and internal resistance, the role of graphene addition was also observed in the prototypes' self-discharge behavior, especially on the charge-redistribution effect under the Open Cell Voltage (OCV) procedure. 20 wt% addition of GNP retained the most charges among the prototypes after being left for 60 minutes in OCV. The self-discharge result was used for the ECM profile fitting. The proposed ECM produces the best circuit fitting on self-discharge among works of literature, especially on the short-term response. This was achieved by introducing an intermediate layer of  $RC$  circuit branch that represents the transitional charge location domain between the Helmholtz layer and the Diffuse layer. The ECM was successfully tested on commercial supercapacitors and the prototypes from this study with an average Root Mean Squared Error of 0.2 %. Applications with a short-term open circuit such as the stop/start features in micro-hybrid vehicles can benefit from this ECM by getting a more accurate State of Charge of the energy storage system used. New insights can be extracted from the ECM as the simulation shows that the graphene addition facilitated the ions' movement into the Helmholtz layer, whereas for the prototype without graphene, most of the ions were restricted at the intermediate layer. The new ECM has the potential to be used as a new characterization method for understanding the supercapacitor's electrode-electrolyte interface.

## خلاصة البحث

تقدم هذه الرسالة بحوث حول مساهمات مواد الجرافين عند دمجها مع قطب المكثف الفائق التقليدي وهو الفحم أجريت التحليلات عن طريق تعريف خصائص المواد وطرق التعريف الكهروكيميائية. اقترحت (AC) النشط يمكن استخدامه كنهج آخر لتعريف الخصائص بالإضافة إلى (ECM) الدراسة نموذجًا جديدًا للدائرة المكافئة إنتاج أفضل نموذج للمكثف الفائق في بيئة نظام إلكتروني افتراضية. أظهرت الدراسات السابقة أن إضافة كمية صغيرة من الجرافين إلى قطب الفحم النشط عززت من أداء القطب في سعة كهربية مخصصة وقللت من المقاومة الداخلية. ومع ذلك ، أفاد بعض الباحثين أن إضافة كمية أكبر من الجرافين ستكون له نتيجة عكسية لأن الجرافين عادةً ما تكون مساحة سطحه المخصصة أقل مقارنةً بالفحم النشط. يستكشف هذا البحث أداء أقطاب المكثف الفائق مع الفحم النشط النقي والجرافين النقي ونسب مختلفة من مركبات الجرافين والفحم النشط (GNP)، تم استخدام نوعين من الجرافين: الجرافين ثنائي الأبعاد باستخدام الصفائح الدموية النانوية للجرافين أشارت النتائج إلى أن الصفائح (GA) والجرافين ثلاثي الأبعاد باستخدام الهلام الهوائي للجرافين أو الإيروجيل الدموية النانوية للجرافين في القطب مرتبطة بالسعة الكهربية المخصصة للنموذج الأولي، ولكن تأثيرها ضئيل على المقاومة الداخلية. من ناحية أخرى ، فإن إضافة نسبة 20٪ من الهلام الهوائي للجرافين أو الإيروجيل إلى القطب تؤدي إلى حصولها على أفضل سعة كهربية ضمن النماذج الأولية المعتمدة على الهلام الهوائي أو الإيروجيل ، و تؤدي زيادة هذه النسبة المتوية إلى تقليل السعة الكهربية. تم أيضًا تسجيل مقاومات داخلية أعلى عند استخدام نسبة مئوية أعلى من هذا الهلام. تم ملاحظة تأثير زيادة الجرافين أيضًا على سلوك التفريغ الذاتي للنماذج الأولية- بالإضافة إلى خاصية السعة الكهربية والمقاومة الداخلية- خاصةً تلك المتعلقة بتأثير إعادة توزيع الشحنة تحت حصلت نسبة إضافة 20٪ من الصفائح الدموية النانوية للجرافين على (OCV) إجراء جهد الدائرة المفتوحة معظم الشحنات مقارنة بالنماذج الأولية بعد تركها لمدة 60 دقيقة في جهد الدائرة المفتوحة. تم استخدام نتيجة بالنظر إلى الدراسات السابقة، فإن هذا النموذج ECM التفريغ الذاتي لمطابقة شكل نموذج الدائرة المكافئة يعد أكثرهم مطابقة لشكل نموذج الدائرة المكافئة عند التفريغ الذاتي، خاصة في حالة الاستجابة قصيرة المدى والتي تمثل مجال موقع الشحنة RC تم تحقيق ذلك من خلال إدخال طبقة وسيطة لفرع دائرة المقاومة والمكثف تم اختبار نموذج الدائرة المكافئة بنجاح على diffuse الانتقالية بين طبقة هلمولتز وطبقة الانتشار الثنائية المكثفات الفائقة التجارية والنماذج الأولية لهذه الدراسة وحصل على متوسط جذر متوسط للخطأ التربيعي يبلغ يمكن للتطبيقات ذات الدائرة المفتوحة قصيرة المدى - كخصائص التوقف /البداء في المركبات الهجينة 0.2% الصغيرة- الاستفادة من نموذج الدائرة المكافئة من خلال الحصول على حالة شحن أكثر دقة للنظام المستخدم لتخزين الطاقة. يمكن استخلاص رؤى جديدة من نموذج الدائرة المكافئة حيث توضح المحاكاة أن إضافة الجرافين سهلت حركة الأيونات في طبقة هلمولتز، أما بالنسبة للنموذج الأولي الخالي من الجرافين ، فكانت معظم الأيونات فيه مقيدة في الطبقة الوسطى. يتمتع نموذج الدائرة المكافئة الجديدة بإمكانية استخدامه كطريقة تعريف جديدة لفهم طريقة تفاعل قطب وإلكتروليتك المكثف الفائق.

## APPROVAL PAGE

The thesis of Abdul Hakim Ab. Rahim has been approved by the following:

---

Nabilah Ramli  
Supervisor

---

Anis Nurashikin Nordin  
Co-Supervisor

---

Mohd Hanafi Ani  
Internal Examiner

---

Muhd Zuazhan Yahya  
External Examiner

---

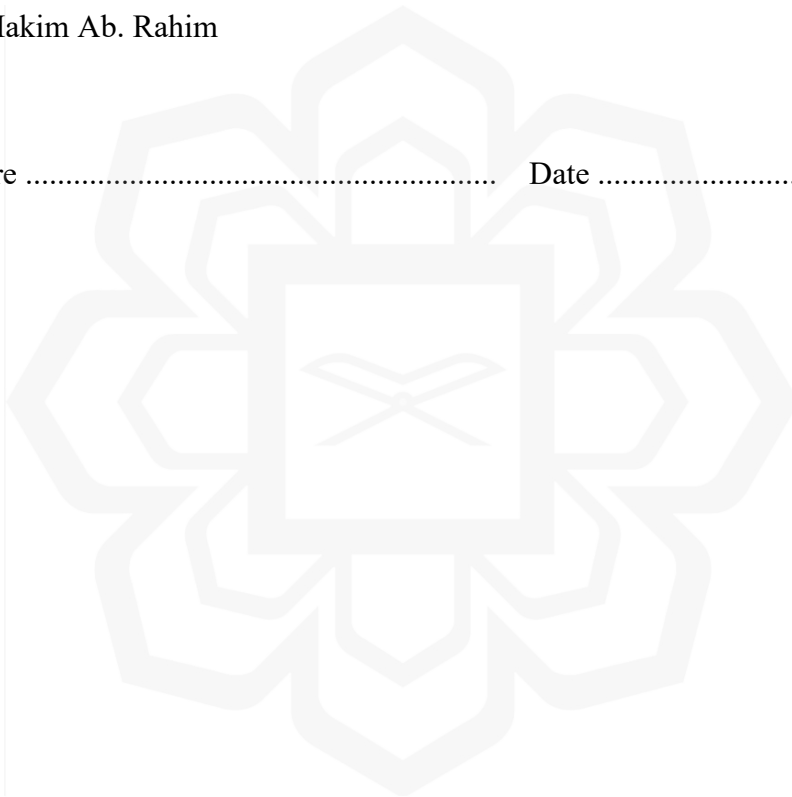
Akram Zeki Kheder  
Chairman

## DECLARATION

I hereby declare that this thesis is the result of my own investigations, except where otherwise stated. I also declare that it has not been previously or concurrently submitted as a whole for any other degrees at IIUM or other institutions.

Abdul Hakim Ab. Rahim

Signature ..... Date .....



**INTERNATIONAL ISLAMIC UNIVERSITY MALAYSIA**

**DECLARATION OF COPYRIGHT AND AFFIRMATION  
OF FAIR USE OF UNPUBLISHED RESEARCH**

**FABRICATION AND CHARACTERIZATION OF  
ACTIVATED CARBON / GRAPHENE SUPERCAPACITOR  
AS AN ENERGY STORAGE DEVICE AND ITS  
EQUIVALENT CIRCUIT MODEL**

I declare that the copyright holder of this thesis is International Islamic  
University Malaysia

Copyright © 2015 by International Islamic University Malaysia. All rights reserved.

No part of this unpublished research may be reproduced, stored in a retrieval system, or transmitted, in any form or by any means, electronic, mechanical, photocopying, recording or otherwise without prior written permission of the copyright holder except as provided below

1. Any material contained in or derived from this unpublished research may only be used by others in their writing with due acknowledgement.
2. IIUM or its library will have the right to make and transmit copies (print or electronic) for institutional and academic purpose.
3. The IIUM library will have the right to make, store in a retrieval system and supply copies of this unpublished research if requested by other universities and research libraries.

By signing this form, I acknowledged that I have read and understand the IIUM Intellectual Property Right and Commercialization policy.

Affirmed by Abdul Hakim Ab. Rahim

.....  
Signature

.....  
Date

## ACKNOWLEDGEMENTS

Firstly, my gratitude to Allah s.w.t who granted me strength and knowledge to finally be able to reach this stage of completion of my thesis.

It is my utmost pleasure to dedicate this work to my dear wife, the queen of my life, Husna Madiha, I can never repay your love, kindness and charity to our family. May Allah reward you with the best place in Jannah for your patience in being by my side through this journey.

To my children, Hanif and Fahad, I wanted to show you the importance of hardships and perseverance in being a part of people who think, people of understanding. I hope I can be a good role model to you in the exploration of knowledge and intelligence. Allahumma faqqihna fiddeen, wa'allimna ta'weel.

To my father, Ab. Rahim and my mother, Rosmawati, my in laws, Chu, my family who granted me the gift of their unwavering belief in my ability to accomplish this goal: thank you for your support and patience.

A special thanks to Dr. Nabilah Ramli who professionally guided me and gave complete support and insightful suggestions in my research direction. Her guidance and enthusiasm are excellent examples and inspiring towards my learning curve in IIUM. My heartfelt appreciation is extended to my co-supervisors, Prof. Dr. Anis Nurashikin Nordin, for the continuous support and encouragement in my Ph.D. journey, and for that, I will be forever grateful

I wish to express my appreciation and thanks to those who provided their ideas, efforts and support for this project. To the members of the VLSI and SDG lab, thank you for being there for me.

May this accomplishment benefit the ummah, and the barakah and reward be the companion for us to Jannah.

# TABLE OF CONTENT

Abstract .....	ii
Abstract in Arabic .....	iii
Approval Page.....	iv
Declaration .....	v
Acknowledgements.....	vii
Table of Content .....	viii
List of Tables .....	xi
List of Figures .....	xiii
List of Abbreviations .....	xx
List of Symbols .....	xxi
<b>CHAPTER ONE: INTRODUCTION .....</b>	<b>1</b>
1.1 Background .....	1
1.2 Problem Statement and Research Gap .....	5
1.3 Research Objectives .....	7
1.4 Research Philosophy .....	7
1.5 Research Scope .....	8
1.6 Research Methodologies .....	8
1.7 Organization of Thesis .....	11
<b>CHAPTER TWO: LITERATURE REVIEW.....</b>	<b>12</b>
2.1 Introduction .....	12
2.2 Energy Density and Power Density rating of supercapacitor .....	12
2.3 Operating Principle of a Supercapacitor .....	13
2.4 Charge location and movements theories .....	18
2.5 Parameters Affecting EDLC Performance.....	22
2.5.1 Operating Voltage Window.....	22
2.5.2 Specific Capacitance .....	26
2.5.3 Equivalent Series Resistance (ESR).....	36
2.6 Fabrication Process of electrodes.....	40
2.6.1 Electrode Additive.....	43
2.6.2 Ball-milling of active material.....	45
2.7 Material Characterization.....	45
2.8 Electrochemical Characterization Techniques.....	49
2.8.1 Electrochemical Impedance Spectroscopy (EIS) .....	49
2.8.2 Cyclic Voltammetry (CV).....	52
2.8.3 Charge Discharge Cycle .....	56
2.8.4 Life Cycle .....	59
2.8.5 Open Circuit Voltage (OCV).....	62
2.9 Equivalent Circuit Models .....	66
2.9.1 Time response-based circuit .....	67
2.9.2 Physics-based circuit .....	69
2.10 Supercapacitors In Power Applications .....	71
2.11 Summary .....	73



<b>CHAPTER THREE: MATERIALS AND METHODS .....</b>	<b>75</b>
3.1 Introduction .....	75
3.2 Materials and Apparatus .....	76
3.3 Material Characterization.....	77
3.3.1 Microscopic Imaging of Materials Surface Profiles.....	77
3.3.2 Molecular Structure Analysis .....	81
3.3.3 Surface and Pores Analysis .....	83
3.4 Design of a supercapacitor .....	86
3.4.1 Electrolyte .....	87
3.4.2 Current Collector .....	87
3.4.3 Electrode.....	88
3.5 Electrode Fabrication .....	90
3.6 Electrode characterization.....	94
3.6.1 Two-point Resistivity Test .....	94
3.6.2 FESEM .....	96
3.7 Prototype Assembly .....	105
3.8 Summary .....	106
<b>CHAPTER FOUR: ELECTROCHEMICAL CHARACTERIZATION OF THE SUPERCAPACITOR.....</b>	<b>107</b>
4.1 Introduction .....	107
4.2 Frequency response test via Electrochemical Impedance Spectroscopy (EIS).....	108
4.3 Electrochemical stability test via Cyclic voltammetry.....	111
4.4 Energy storing capability test via Charge-discharge.....	114
4.4.1 Constant Current Charging/Discharging (Chronopotentiometry) .....	114
4.4.2 Constant Voltage Charging (Chronoamperometry) .....	116
4.4.3 Constant Current - Constant Voltage Combination Charging 118	
4.5 Open Circuit Voltage (OCV) .....	120
4.6 Result and Discussion .....	122
4.6.1 Prototypes Capacitance Trend.....	122
4.6.2 Internal resistance.....	137
4.6.3 Self-discharge .....	140
4.6.4 Life Cycle Comparison .....	146
4.7 Energy Density and Power Density .....	153
4.8 Summary .....	154
<b>CHAPTER FIVE: EQUIVALENT CIRCUIT MODEL.....</b>	<b>156</b>
5.1 Introduction .....	156
5.2 Proposed Equivalent Circuit Model and Ionic Layer Representation.....	158
5.3 Mathematical expression and simulation.....	159
5.4 Prototype Simulation fitting.....	162
5.5 ECM fitting procedure .....	165
5.6 Validation of Equivalent Circuit Model.....	166
5.6.1 Validation of ECM on Commercial Device .....	166
5.6.2 Validation of ECM under External Load .....	168

5.6.3	Validation of ECM for Different Charging Approaches....	169
5.7	prototypes trends: insights from the ECM .....	171
5.7.1	GNP-based Prototype Fitting .....	172
5.7.2	GA-based Prototype Fitting.....	174
5.8	Summary .....	177
<b>CHAPTER SIX:CONCLUSION AND RECOMMENDATION .....</b>		<b>179</b>
6.1	Conclusion .....	179
6.2	Fabrication Limitation.....	182
6.3	Recommendation.....	184
<b>REFERENCES.....</b>		<b>186</b>
<b>APPENDIX I: SURFACE AREA ANALYSIS REPORT .....</b>		<b>205</b>
<b>APPENDIX II: ECM MATLAB CODING .....</b>		<b>208</b>



## LIST OF TABLES

Table 2-1: Type Of Electrolytes And Their Properties (Pandolfo et al., 2013)	23
Table 2-2: Ions Sizes And Their Conductivity (Zhong et al., 2015)	28
Table 2-3: Comparison of AC, Graphene and AC/Graphene Composites Electrode Reported In Literature	34
Table 2-4: Various Types Of Carbon and its Properties (Lemine et al., 2018)	39
Table 3-1: Materials Used for Supercapacitor Prototype	76
Table 3-2: Equipments Used for Fabrication Process	76
Table 3-3: Equipments Used FOR Characterization Process	77
Table 3-4: Intensity Peak Values for Raman Spectrum for AC, GA and GNP	82
Table 3-5: Specific Surface Area (SSA) According to BET, BJH, and DFT Estimation Method	84
Table 3-6: Specimens of Different AC, Graphene, and Additive Percentages.	88
Table 3-7: Calculated Theoretical SSA for Each Composite Electrode	89
Table 4-1: Test Descriptions and the Characterized Parameters Summary	108
Table 4-2: Specific Capacitance Value for GNP based Prototypes	125
Table 4-3 : Specific Capacitance Value for GA based Prototypes	127
Table 4-4: The Measured Parameters from the Constant Voltage Procedure	129
Table 4-5: Specific Capacitance Recorded for GNP Specimens from the Voltage-hold Procedure	131
Table 4-6: Specific Capacitance Recorded for GA Specimens from Voltage-hold Procedure	133
Table 4-7: ESR Recorded for GNP Prototypes	139
Table 4-8: ESR Recorded for GA Prototypes	139
Table 4-9: OCV Procedure Results for GNP-based Prototypes	143
Table 4-10: OCV Procedure results for GA-based Prototypes	144
Table 5-1: Each Components Representation in the S-Domain Parameters	160

Table 5-2: Fitted Parameters for Constant Current Charging and Multiple Charging Approach	171
Table 5-3: Fitted Parameters for GNP Prototypes	173
Table 5-4: Fitted Parameters for GA Prototypes	175



## LIST OF FIGURES

Figure 1.1: Specific Power and Specific Energy for Supercapacitors Compared to Batteries (Xie et al., 2018)	2
Figure 1.2: Flow Chart of Research Methodology	10
Figure 2.1: Conventional Parallel Plate Capacitor	14
Figure 2.2 (a) A Cross-section and Simplified Physical Structure of a Supercapacitor, (b) Common Simplified Supercapacitor Equivalent Circuit Model Based on its Physical Structure.	16
Figure 2.3: The More Complex Capacitance and Resistance Network Going Deeper in a Straight Simplified Pore (Pandolfo et al., 2013).	18
Figure 2.4: Schematic of the Electric Double Layer Structures Based on Each Theory at The Electrode-Electrolyte Interface (Wang et al., 2011)	20
Figure 2.5: Aligned Graphene Layers as Parallel Planes for Ease of Ion Movements (Bose et al., 2012).	30
Figure 2.6: Specific Capacitance Performance Compared to its (a) Mass Loading (Wang et al., 2016) or (b) Coating Thickness (Chmiola et al., 2010)	36
Figure 2.7: Fabrication of Supercapacitors. (a) Commercial Supercapacitor Device Rolled Components (b) Supercapacitor Cell in Compressed Casing (Stoller et al., 2008) (c) Flexible Electrode Using Textile Method (Hu et al., 2010) ,(d) Graphene Layers on The Surface of Metal Foam (Zhang et al., 2016), (e) 3D-Printed Graphene-Based Electrode With Controlled Size and Shape (Yao et al., 2019), (f) Graphene Micro Supercapacitor Electrode (El-Kady et al., 2015).	42
Figure 2.8: An Image of Pores from Palm Shell Activated Carbon on the Scale of Micrometer (Maarof et al., 2017)	46
Figure 2.9: Raman Spectra for Single-Layer Graphene VS. Bulk Graphite (Childres et al., 2013)	47
Figure 2.10: (a): Classification of Physisorption Isotherms (Thommes et al., 2015) and (b): Example of Physisorption Isotherm (a) and Pore-Size Distribution (b) (Li et al., 2011).	48
Figure 2.11: (a) Equivalent Circuit With $R_s$ = Series Resistance, $C_{dl}$ =Double Layer Capacitance, $R_T$ = Charge Transfer Resistance and $W$ = Warburg Impedance. (b) Nyquist Plot Shows the High Frequency	

(HF) and Low Frequency (LF) Response (Taberna & Simon, 2013)	50
Figure 2.12: Physical Interpretation of EDLC Activity Based on Nyquist Plot by Mei et al. (2018)	51
Figure 2.13: CV Profile for Cathode, Anode, and Complete Cell for 3 V and 3.5 V Voltage Limit (Aken et al., 2015)	53
Figure 2.14: CV Profiles of an AC-Based Electrode Showing Changing Profile Shape as the Scan Rate Increase (Fletcher et al., 2014)	54
Figure 2.15: CV Profiles with Different Scan Rate and Their Subsequent Specific Capacitance Value (Zequine et al., 2016).	55
Figure 2.16:(A) Typical Constant Current Charging Profile with Several Current Magnitude Comparisons (Wang et al., 2011) (B) Zoomed-In View to Show Voltage Drop (Zhang et al., 2015)	56
Figure 2.17: Simple RC Circuit Contains One Element of $C$ and $R$	57
Figure 2.18: Typical Current Profile as Constant Voltage Charging Taking Place (Maarof et al., 2017)	58
Figure 2.19: Constant Current Charging Followed by Constant Voltage Charging. Here the Author Varies the 'Holding' Time of Constant Voltage Charging (Zhang et al., 2015)	59
Figure 2.20: Capacitance Retention After Charge-Discharge Cycles By (a) Chiam et al., (2018) and (b) Tsai et al., (2017)	60
Figure 2.21: SEM Images of Positive and Negative Electrodes After Cycle Test at a Different Voltage (Ishimoto et al., 2009).	62
Figure 2.22: Voltage Decay at OCV with Different Voltage Charging Duration. From Top: 30, 20, 15, 10, 8, 6, 4 and 2s (Fletcher et al., 2014).	63
Figure 2.23: Voltage Decay After Different Charging Voltage (Subramanian et al., 2018).	64
Figure 2.24: (a) Diffusion-Based Plot and (b) Ohmic-Based Plot	65
Figure 2.25: (a)RC Parallel Model With Fast, Medium and Slow-Term Response Branch (Shi et al., 2008) and (b)RC Dynamic Model, a Combination of Parallel and Series Model with $R_s$ Represents Internal Resistance (Zhang et al., 2015)	67
Figure 2.26: Two Advanced Equivalent Circuit Models Based on Time-Response of a Supercapacitor (a) Zubieta and Bonert's Model, (b) Universal (Fletcher et al., 2014), (c) General RC Parallel by (Shi et al., 2008)	68

Figure 2.27: Two Examples of Equivalent Circuit Models Based on the Physics Theory of a Supercapacitor, (a) by Kubarowitz (2017) and (b) by Kang et al., (2014)	70
Figure 2.28: Improved Ladder Model with Controlled Current Source (B. Wang et al., 2020)	71
Figure 2.29: Fitting Simulation from Sedlakova Model and (a)Zubieta's (Kuprowitz, 2017) and (b)Varied Leakage Resistance) (Saha et al., 2017)	71
Figure 3.1: Activated Carbon in the Scale of 10 $\mu\text{m}$	78
Figure 3.2: Activated Carbon in the Scale of 5 $\mu\text{m}$	78
Figure 3.3: GA in the Scale of 10 $\mu\text{m}$	79
Figure 3.4: GA Particle Thickness and Surface Layers	79
Figure 3.5: Graphene Nanoplatelet in the Scale of 10 $\mu\text{m}$	80
Figure 3.6: Graphene Nanoplatelet in the Scale of 1 $\mu\text{m}$	80
Figure 3.7: Carbon Black in the Scale of 1 $\mu\text{m}$	81
Figure 3.8: Raman Intensity for AC, GA and GNP	82
Figure 3.9: Physical Adsorption Isotherm for (a )AC, (b) GNP and (c) GA	84
Figure 3.10: Pore Distribution for (a) AC, GNP, and GA and (b) a Zoomed Plot for GA.	86
Figure 3.11: The Illustration of a Used Electrochemical Cell Configuration	87
Figure 3.12: Electrodes Composition Summary for All Specimens	89
Figure 3.13: Calculated SSA for (a) GNP and (b) GA Electrodes	90
Figure 3.14: Flowchart for Fabrication and Characterization of Prototypes	91
Figure 3.15: Original Shape of Graphene Aerogel	92
Figure 3.16: Ball Milling Machine Used for Grinding GA	92
Figure 3.17: (a) Mixed Active Material with CB, (b) Solution with Solvent and Active Material Mix, (c) Resulting Powder Paste Mix.	93
Figure 3.18: (a) Hydraulic Pressing of Mold Contains Active Material and Current Collector, (b) the Fabricated Electrode.	93
Figure 3.19: Electrode Setup for 2-Points Probe	94

Figure 3.20: Electronic Resistance for Specimens in $\Omega/\text{Cm}$	95
Figure 3.21: Surface Morphology of (a) AC, (b) GA20, (c) GA80, (d) GNP20, (e) GNP80 at the $\times 5000$ Magnification.	97
Figure 3.22: AC Electrode at $\times 30,000$ Magnification	98
Figure 3.23: Pores and CB on AC Electrode	99
Figure 3.24: Binder Layer Covering the Surface of Active Material	99
Figure 3.25: GA80 Surface Area at $\times 5,000$ Magnification	100
Figure 3.26: Uneven CB Dispersion on GA80 Electrode	101
Figure 3.27: GNP80 Electrode Surface	102
Figure 3.28: GNP80 Surface at the Edge of the Electrode	102
Figure 3.29: GNP20 Electrode Surface at $\times 30,000$ Magnification	103
Figure 3.30: Surface Contours at the Edge of GNP20 Electrode	104
Figure 3.31: Current Collector and Electrode Active Material Interface at (a) $\times 65$ , (b) $\times 6000$ and (c) $\times 1500$ Magnification Factor.	105
Figure 3.32: The Assembly of the Complete Cell Electrode Sandwich	106
Figure 4.1: The Setup for a Full Cell Procedure Using PGSTAT302 Autolab Equipment	109
Figure 4.2: Nyquist Plot for GA-Based Prototypes	110
Figure 4.3 Nyquist Plot for GNP-Based Prototypes	110
Figure 4.4: The Interpretation of Nyquist Plot on GA60 Impedance Result	111
Figure 4.5: CV Plot for GA Prototypes at 0.001 V/s, 0.01 V/s, and 0.1 V/s Scan Rate	112
Figure 4.6: CV Plot for GNP Prototypes at 0.001 V/s, 0.01 V/s, and 0.1 V/s Scan Rate	113
Figure 4.7: Charge-Discharge Curves for GNP Specimens at 10 mA/g Current with Voltage Drop Shown in the Red Circle.	115
Figure 4.8: Charge-Discharge Curves for GA20 Specimens at 10, 20, 30, and 50 mA/g Currents.	115
Figure 4.9: Current Response for Constant Voltage Charging at 1 V for All GNP Based Specimen	117



Figure 4.10: Voltage (Black) and Current (Red) Profile for Specimen GNP20 Charged at 4 mA Current, Hold at 1 V Voltage and Discharge at 4 mA.	118
Figure 4.11: Discharge Profiles from the Different Charging Approaches of GNP80 Prototype at 20 mA/g Current Density.	119
Figure 4.12: Self-Discharge for GNP and GA Specimens From OCV Test	121
Figure 4.13: Specific Capacitance Comparison for All Prototypes from EIS Procedure	122
Figure 4.14: Specific Capacitance for All Prototypes for Different Scan Rates in Logarithmic Scale	123
Figure 4.15: Specific Capacitance for GNP Electrodes for All Current Magnitude	125
Figure 4.16: Specific Capacitance for GNP-Based Prototypes According to Current Density	126
Figure 4.17: Specific Capacitance for GA Electrodes for All Current Magnitude	127
Figure 4.18: Specific Capacitance for GA-Based Prototypes According to Current Density	128
Figure 4.19: Specific Capacitance Using Constant Voltage Method for All Prototype (Solid), Compared to The Specific Capacitance from Constant Current Method (Dashed).	129
Figure 4.20: Specific Capacitance Comparison Between Voltage-Hold (Black) and Constant Current (Red) for GNP Specimens	131
Figure 4.21: The Performance of GNP-Based Prototypes From Constant Current + Constant Voltage (Solid Line) and Constant Current (Dashed Line) According to Current Densities	132
Figure 4.22: Specific Capacitance Comparison Between Voltage-Hold (Black) and Constant Current (Red) for GA Specimens	132
Figure 4.23: The Performance of GA-Based Prototypes from Constant Current + Constant Voltage (Solid Line) and Constant Current (Dashed Line) According to Current Densities	134
Figure 4.24: The Specific Capacitance Trend in Comparison to Specific Surface Area Estimation for GNP and GA Prototypes	135
Figure 4.25: AC Electrode's Pore Opening may be Blocked by CB and PTFE	136

Figure 4.26: $R_{electrode}$ and $R_{electrolyte}$ for GA and GNP Prototypes	137
Figure 4.27: ESR for GA and GNP Electrodes	139
Figure 4.28: Diffusion Activity Slope for GA and GNP Prototypes	141
Figure 4.29: Self-Discharge Plot for GNP Prototypes According to (a) Voltage Percentage, (b) $V$ Vs. $\log T$ for Faradaic Discharge Test, (c) $\ln V$ Vs. $T$ for Ohmic Test, and (d) $V$ Vs. $\sqrt{T}$ for Charge Redistribution	142
Figure 4.30: Self-Discharge Plot for GA Prototypes According to (a) Voltage Percentage, (b) $V$ Vs. $\log T$ for Faradaic Discharge Test, (c) $\ln V$ Vs. $T$ for the Ohmic Test, and (d) $V$ Vs. $\sqrt{T}$ for Charge Redistribution.	142
Figure 4.31: Charge Redistribution and Ohmic Leakage Slopes Comparison Between GNP-Based and GA-Based Prototypes.	144
Figure 4.32: Leakage Resistance from OCV Procedure	145
Figure 4.33: Capacitance Retention and ESR Increment for GNP (a and b) and GA (c and d) for 1000 Cycles.	147
Figure 4.34: Fresh (Top) and Cycled (Bottom) GNP80 Electrode Comparison. Used Electrode Shows Some Parts with Lumped and Curvy Edges (Circled) as a Sign of Affected Particle Structure	150
Figure 4.35: Fresh (Top) and Cycled (Bottom) GA80 Electrode Comparison. The Used Electrode Shows the Shape of Damaged Edges Circled.	151
Figure 4.36: Fresh (Top) and Cycled (Bottom) AC Electrode Comparison. The Used Electrode Shows the Shape Of Damaged Edges Circled.	152
Figure 4.37: Ragone Plot for GNP-Based and GA-Based Prototypes	154
Figure 5.1: (a) The Cross-Section Showing Electrode-Electrolyte Interface, which Correlates with the Proposed Equivalent Circuit Model Representation in (b).	159
Figure 5.2: The ECM with Components Represented as the Impedance Blocks.	160
Figure 5.3: Equivalent Impedance Simplification for All the Branches	161
Figure 5.4: The AC Prototype Charge-OCV Plot Fitting with 0.17% RMSE.	163
Figure 5.5: The OCV Profile for Fitting for Simulation with an Intermediate Branch (Left) and Without an Intermediate Branch (Right).	164
Figure 5.6: Fitting from Sedlakova's ECM on Commercial Supercapacitor	164

Figure 5.7: DRL 10 F (Left) and IOXUS 350 F (Right) Commercial Supercapacitor Device	166
Figure 5.8: Simulation Result for 10 Farads DRL Device	166
Figure 5.9: Simulation Result for 350 Farads IOXUS Device at 2.5V.	167
Figure 5.10: PSPICE Model Setup for the ECM External Load Validation	168
Figure 5.11: ECM Experimental and Simulation Comparison with 100 $\Omega$ and 10,000 $\Omega$ External Resistor.	169
Figure 5.12: Constant Current Charging and OCV Simulation Fitting with 0.05% RMSE Value	170
Figure 5.13: Constant Current Followed by Constant Voltage Charging and OCV Simulation Fitting with 0.05% RMSE Value	171
Figure 5.14: Experimental VS. Simulated Specific Capacitance for GNP Prototypes. Additional Capacitance Data from Each Branch are also Presented.	172
Figure 5.15: Time Constant for Intermediate (Left Axis) and Diffuse (Right Axis) Branch for GNP-Based Prototypes.	174
Figure 5.16: Experimental VS. Simulated Specific Capacitance for GA Prototypes	175
Figure 5.17: Capacitance Percentage in Each Ionic Layer	176
Figure 5.18: Time Constant for Intermediate (Left Axis) and Diffuse (Right Axis) Branch for GA-Based Prototypes.	177
Figure 6.1: (a) 45 mg/cm <sup>2</sup> Material Loading and (b) 15 mg/cm <sup>2</sup> Material Loading (Right) Electrode Comparison	183

## LIST OF ABBREVIATIONS

wt%	Weight percentage
AC	Activated Carbon
BET	Brauner-Emmett-Teller
BJH	Barret-Joyner-Halenda
BTS	Battery Testing System
CB	Carbon Black
CV	Cyclic Voltammetry
ECM	Equivalent Circuit Model
EDLC	Electrical Double Layer Capacitance
EIS	Electrochemical Impedance Spectroscopy
ESR	Equivalent Series Resistance
FESEM	Field Emission Scanning Electron Microscope
GA	Graphene Aerogel
GNP	Graphene Nanoplatelets
KOH	Potassium Hydroxide
OCV	Open Circuit Voltage
RC	Resistance-Capacitance
RMSE	Root Mean Squared Error
SEM	Scanning Electron Microscope
SSA	Specific surface area

## LIST OF SYMBOLS

$A$	Surface area (m <sup>2</sup> /g)
$C$	Capacitance (Farad)
$c$	Concentration of ion
$d$	Distance (m)
$D$	Diffusion coefficient
$E$	Energy Density (Wh/kg)
$F$	Faraday Constant
$f$	Frequency
$I$	Current (A)
$k_B$	Boltzmann constant
$m$	Mass (kg)
$N$	Molar flux
$P$	Power Density (W/kg)
$Q$	Charge
$R$	Resistance ( $\Omega$ )
$R$	Gas Constant
$T$	Temperature ( $^{\circ}\text{C}$ )
$u$	Fluid Velocity
$V$	Voltage (V)
$v$	Scan rate (V/s)
$z$	Electron valance
$Z$	Impedance ( $\Omega$ )
$\varepsilon$	Permittivity
$\lambda$	Deby length
$\Phi$	Electric Potential (V)
$\Gamma$	Tortuosity

# CHAPTER ONE

## INTRODUCTION

### 1.1 BACKGROUND

Supercapacitors, batteries, and fuel cells are the three categories of electrochemical energy storage. Batteries are the most common device that is used in many applications, from automotive to personal electronics. In this age of fast technologies, supercapacitors have started to get increasing attention as an alternative energy storage device because of their well-known ability of rapid charge and discharge. In addition to much higher power density performance than the battery, the supercapacitor's high life cycle is attractive to minimize maintenance costs.

The current commercial supercapacitor can store a very high amount of charge up to several thousands of Farads. Activated Carbon (AC) is commonly used as the primary material of the device's electrodes. This porous carbon comprises of an extensive surface area that provides more space for the charge to occupy. However, as can be seen from Figure 1.1, the energy density of a supercapacitor is still 1/10<sup>th</sup> of battery energy density (Xie et al., 2018). Many approaches are being explored to increase energy density, including introducing new active materials such as Carbon Nanotube (CNT) and Graphene.

Graphene is a new carbon material that has the potential to boost supercapacitor to a new level of the energy storage device. Graphene is said to have much better electronic properties compared to AC but is more expensive to produce in bulk. The

limited technology to attain low-cost graphene is the barrier for graphene to take over as the leading material for the supercapacitor's electrode (Lemine et al., 2018).

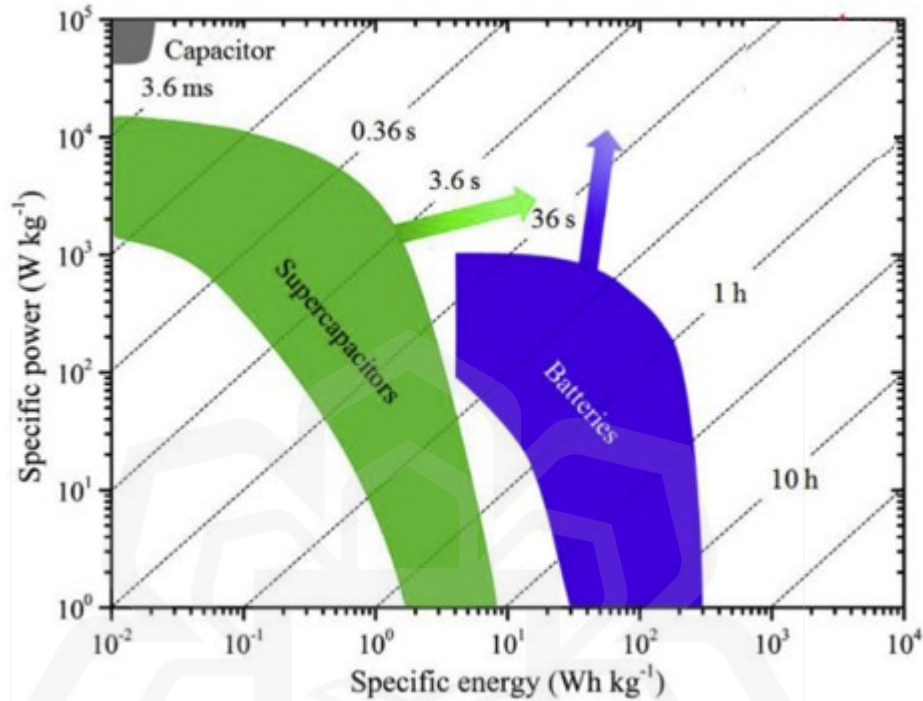


Figure 1.1: Specific power and specific energy for supercapacitors compared to batteries (Xie et al., 2018)

Many works of literature have shown that graphene-based electrode has better capacitance than the AC electrode even though graphene's theoretical specific surface area is 2675 m<sup>2</sup>/g (Ke et al., 2016), much lower compared to AC which is as high as 4000 m<sup>2</sup>/g (H. Chen et al., 2012). Since the capacitance of a supercapacitor is a function of the specific surface area (SSA) of the active material on the electrode (Simon et al., 2013), this raises the question of whether the surface area estimation method used is a correct tool to estimate the capacitance potential, or what are the advantages of graphene's surface area that are more suitable for ion adsorption?

Many types of graphene are available in the research market ranging from 0-Dimensional (0-D) to 3-Dimensional (3-D) graphene (Ke et al., 2016). A 0-D or

graphene dots and particles are in the form of powder; 1D graphene is produced in the structure of the fibrous yarn, 2D graphene in the shape of carbon film, and 3D graphene is produced in the form of aerogels or foam-template. The different graphene synthesis methods result in various grades of graphene purity and affect its desired properties.

Graphene also faces another physical challenge as graphene sheets tend to agglomerate and restack because of the van der Waals forces (Atif et al., 2016). This phenomenon causes the layers of graphene material to rejoin, and the pores are blocked, preventing maximum ion adsorption on all the available surfaces. Graphene powders and films have a higher tendency to aggregate compared to the 3D Graphene Aerogels (GA) due to GA's hexagonally bonded carbon atom structure (Mao et al., 2018). The opening of layers in GA can better facilitate ion movements compared to dense and packed layers of graphene in powders or films.

There are a few works that reported a combination of the AC and graphene as the electrode materials in order to improve the device capacitance and internal resistance. The graphene was used either to act as the conductive agent to enhance the performance of the supercapacitor (Zhang et al., 2017) or as the primary material together with the AC (Azam et al., 2015). While the addition is expected to improve the device's performance, that is not always the case since there are trade-offs between the combined material's advantages and drawbacks.

Besides capacitance and internal resistance, self-discharge is another characteristic that is less focused and reported for a supercapacitor. When a fully charged supercapacitor is left in an open circuit, the device will gradually lose its charge between 10 – 20 % within a few days (Gualous et al., 2013). The decline in supercapacitor voltage in an open circuit creates an unreliable factor that affects the energy-storing task performance (Conway, 1999). Even though the self-discharge